Organic & Biomolecular Chemistry

RSC Publishing

PAPER

View Article Online
View Journal | View Issue

Cite this: *Org. Biomol. Chem.*, 2013, **11**, 509

Protein secondary structure mimetics: crystal conformations of α/γ^4-hybrid peptide12-helices with proteinogenic side chains and their analogy with α- and β-peptide helices†

Sandip V. Jadhav, Anupam Bandyopadhyay and Hosahudya N. Gopi*

Numerous strategies have been developed to mimic the α-helical secondary structure using hybrid peptides containing non-natural amino acids. In contrast to the β- and α/β-hybrid peptides, very little is known about the folding patterns of hybrid peptides containing γ^4-amino acids. Here we report the solid phase synthesis and crystallographic insight into the secondary structures formed by 1 : 1 alternating α/γ^4-hybrid peptides. The crystal conformations suggest that heptapeptides **P1**, **P2** and **P3** adopted the 12-helix conformation with backward consecutive 1←4 H-bonds [C═O(i)···H–N (*i* + 3)]. In comparison with α-, β- and γ-peptides, the distinct projection of side-chains was observed along the helical cylinder. In contrast to the peptide containing stereochemically constrained α-amino acid Aib (**P1**), the peptide with complete proteinogenic side-chains (**P3**) displayed organized side chain–side chain interactions between the antiparallel helices in crystal packing. The analogy of the α/γ^4-hybrid peptides with 3_{10}-helix, α-helix and β-peptide 12-helix suggests that the internal H-bonding pattern and macrodipole were analogous to the α- and β-peptide helices. In addition, helical parameters were found to be very similar to that of β-peptide 12-helices.

Received 14th September 2012,
Accepted 19th November 2012

DOI: 10.1039/c2ob26805a

www.rsc.org/obc

Introduction

Helices constitute the major secondary structural components of proteins and often play a crucial role in mediating protein–protein and protein–nucleic acid (DNA and RNA) interactions.[1] Disrupting these interactions with isolated helical structures is of paramount importance not only to understand the biological consequences of the interactions but also from the perspective of drug design. Several approaches have been developed to mimic the short and stable α-peptide helices including covalent cross-linkage of amino acid side-chains,[2] utilization of C–C covalent bonds as an intramolecular H-bond surrogate [3] or non-peptidic organic templates.[4] The recent exponential growth of β- and γ-peptide foldamers provides an alternative and straightforward approach to mimic protein secondary structures.[5] The advantage of hybrid peptides with a heterogeneous backbone (peptides with α and other β- and γ-amino acids) is that a variety of hydrogen bonded helical structures can be generated by varying the amino acid sequence patterns. Extensive investigations revealed that β-, γ-, mixed α/β- and α/γ-hybrid peptides adopt various ordered helical conformations including 14-, 12-, 10/12-, 9- and 8-helices. In contrast to the 14-helical conformations of cyclic β-amino acids with a six membered ring constraint (*trans*-2-aminocyclohexane carboxylic acid) [6] and acyclic β-amino acids (β^3- and β^2-amino acids),[5a] the homooligomers of cyclic β-amino acids with four (*trans*-2-aminocyclobutane carboxylic acid),[7] five (*trans*-2-aminocyclopentane carboxylic acid and its derivatives)[8] membered ring constraint and a bicyclo[2.2.1] heptene skeleton[9] displayed the 12-helical conformations. The cyclic ring constraints of these amino acids preorganize the β-peptide backbone to adopt helical conformations. In addition, Gellman *et al.*[10] and others[11] have demonstrated the inhibitions of protein–protein interactions using 12-helical scaffolds. Further, Lee *et al.* showed the exceptional self-assembly behaviour of the 12-helical peptides.[12] Recent theoretical results suggest that the 12-helical conformation is not unique to the homooligomers of cyclic β-amino acids, the heterooligomers composed of 1 : 1 α- and unsubstituted γ-amino acids

Department of Chemistry, Indian Institute of Science Education and Research, Dr. Homi Bhabha Road, Pune-411 008, India. E-mail: hn.gopi@iiserpune.ac.in

†Electronic supplementary information (ESI) available: Details of chemical synthesis, characterization and crystallographic details of γ^4-Phe and peptides **P1**, **P2** and **P3**, average helical parameter table, hydrogen bond parameters and torsional angle tables, HPLC traces, CD analysis and complete spectroscopic data for all compounds. CCDC . CCDC reference numbers 901427–901430. For ESI and crystallographic data in CIF or other electronic format see DOI: 10.1039/c2ob26805a

have shown to adopt 12-helix.[13] In their experimental work, Balaram and colleagues[14] and Gellman *et al.*[15] have shown 12-helical conformations in α/γ-hybrid peptides containing acyclic γ-amino acids and cyclic γ-amino acids, respectively. Recently, we have shown the 12-helical organizations in the short α/γ^4-hybrid peptides obtained through the direct transformation from α/vinylogous hybrid peptides using catalytic hydrogenation.[16] In all these cases stereochemically constrained amino acids have been used to induce the helical conformation in the peptides. As proteinogenic amino acid side chains play a pivotal role in biomolecular interactions, we sought to investigate structural properties of α/γ^4-hybrid peptides with complete proteinogenic side chains. Herein, we are reporting the solid phase synthesis, single crystal conformations of α/γ^4-hybrid heptapeptides Ac-Aib-γ^4Phe-Aib-γ^4Phe-Aib-γ^4Phe-Aib-$CONH_2$ (**P1**), Ac-Ala-γ^4Phe-Ala-γ^4Phe-Ala-γ^4Phe-Aib-$CONH_2$ (**P2**), Ac-Ala-γ^4Phe-Ala-γ^4Phe-Ala-γ^4Phe-Ala-$CONH_2$ (**P3**) and their analogy with 3_{10}-helix, α-helix and β-peptide 12-helices.

Results and discussion

Design and synthesis of α/γ^4-hybrid peptides

To understand whether α/γ^4-hybrid peptides can fold into helical conformations without any stereochemical constraint, we designed three heptapeptides **P1**, **P2** and **P3**. We have utilised γ^4-Phe in combination with α amino acids to synthesize α/γ^4-hybrid peptides. The solid phase compatible Fmoc-γ^4-Phe was synthesized through the catalytic hydrogenation of the benzyl ester of N-Cbz-protected α, β-unsaturated γ-phenylalanine followed by the Fmoc-protection as shown in Scheme 1. In addition, single crystals of free amino acid γ^4-Phe obtained as an intermediate in the process of the reaction yield the structure shown in Fig. 1. The advantage of this method is that the γ^4-amino acids can be directly incorporated into the peptide sequence using solid phase synthesis. The stereochemically constrained helix favouring α,α-dialkyl amino acid (Aib)[17] was used as an α-amino acid in 1 : 1 alternating α/γ^4-hybrid peptide **P1**. In the case of **P2**, except the C-terminal Aib, all other Aibs are replaced with L-Ala. In **P3** all Aibs are replaced with L-Ala. The sequences of these peptides are shown in Scheme 2. All peptides were synthesized on a Knorr Amide MBHA resin using the standard Fmoc-chemistry protocol. The coupling reactions were mediated by HBTU/HOBt coupling conditions.

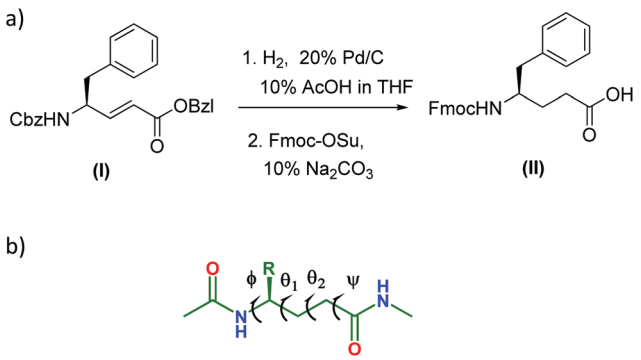

Scheme 1 (a) Synthesis of Fmoc-γ^4-Phe and (b) local conformational variables of γ^4-amino acids.

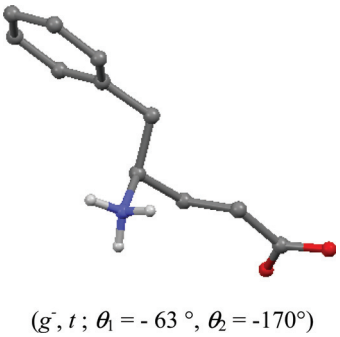

$(g^-, t\ ;\ \theta_1 = -63\ °,\ \theta_2 = -170°)$

Fig. 1 X-ray structures of free γ^4-Phe. Conformation and torsional values are given below.

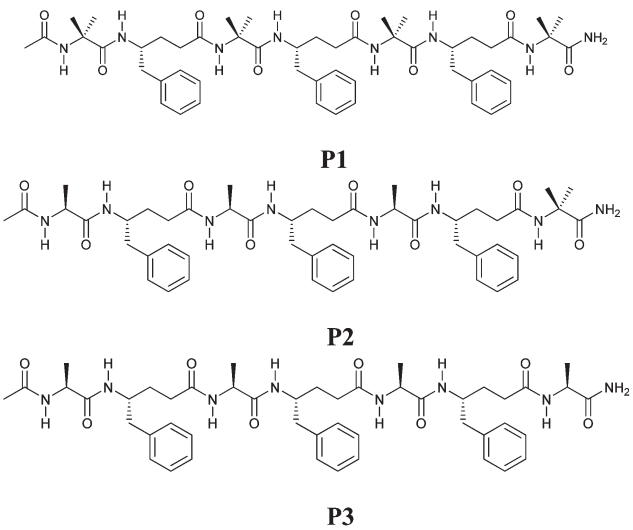

Scheme 2 α/γ^4-Hybrid peptides **P1**, **P2** and **P3** synthesized using solid phase peptide synthesis.

Crystal structures are very important in understanding the helical parameters such as residue-per-turn, rise-per-turn, helical radius and the projection of amino acid side-chains in the newly designed peptides. Keeping this in mind, we attempted to grow the X-ray quality crystals from all three peptides in various solvent combinations.

Crystal conformations of α/γ^4-hybrid peptides

Single crystals of peptides **P1** and **P2** were obtained from the slow evaporation of aqueous methanol–trifluoroethanol solution. The suitable X-ray quality single crystals of **P3** were obtained after repeated attempts of slow evaporation from aqueous methanol solution. The X-ray structures of all three peptides are shown in Fig. 2. Instructively, all three peptides adopted right-handed helical conformations with consecutive

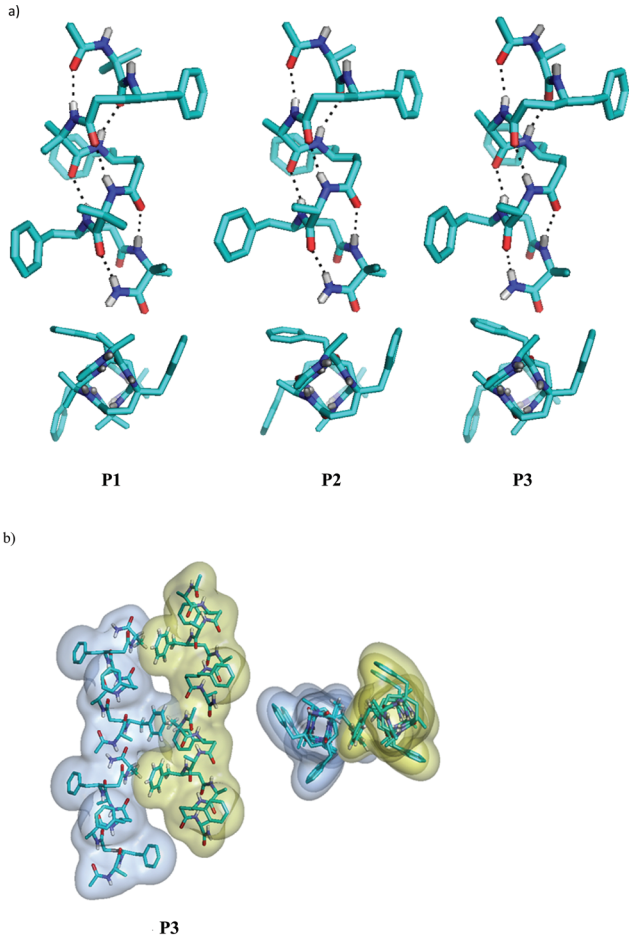

Fig. 2 (a) X-ray structures of **P1**, **P2** and **P3**. Top view is shown in the lower plane. (b) The lateral interaction of anti-parallel 12-helices of **P3** in the crystal packing and the top view of 12-helix **P3** are also shown.

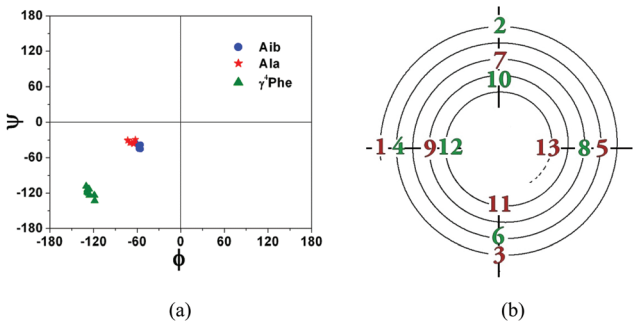

Fig. 3 (a) A two dimensional Ramachandran type plot depicting ϕ and ψ values in the α/γ^4-hybrid peptides. The torsional variables θ_1 and θ_2 are kept constant as they always take the values close to 60° in the hybrid helices. (b) The helical wheel diagram depicting side chain projection in α/γ^4-hybrid peptides. α-Amino acids are shown in red while γ^4-amino acids are shown in green.

12-membered H-bonds [C═O(i)···H–N(i + 3), 12-atom ring H-bonds]. Similar to the native α-amino acid helices, α/γ^4-hybrid helices displayed the backward H-bonding directionality and subsequent macrodipole. The 12-helical conformation in all the α/γ^4-hybrid peptides is stabilized by six consecutive 1←4 [C═O(i)···H–N(i + 3)] intramolecular H-bonds. Both a C-terminal amide and an N-terminal Ac-group are involved in the intramolecular H-bonds. Additionally, the packing mode of individual peptides revealed that each helical peptide is interconnected with the other helical peptides in a head-to-tail fashion through four intermolecular H-bonds. The inter- and intramolecular H-bond parameters of all three peptides are tabulated in the ESI.† Inspection of the crystal structure of **P1** reveals that Aib residues adopted right handed helical conformations by having average ϕ and ψ values −58 ± 3° and −40 ± 5°, respectively. The dihedral angles of γ^4-Phe residues were measured by introducing two additional variables θ_1 (N–C$_\gamma$–C$_\beta$–C$_\alpha$) and θ_2 (C$_\gamma$–C$_\beta$–C$_\alpha$–C) as shown in Scheme 1b. In contrast to the amino acid structure, the stereochemical analysis of γ^4-Phe residues in all the peptides reveals that they adopted *gauche*$^+$, *gauche*$^+$ (g^+, g^+, $\theta_1 \approx \theta_2 \approx 60°$) local conformations about the C$_\beta$–C$_\gamma$ and C$_\alpha$–C$_\beta$ bonds. The average ϕ and ψ values of γ^4-residues were found to be 125 ± 7 and −118 ± 10°, respectively. The H-bonding pattern between the 1←4 residues and directionality of the H-bond in all α/γ^4 hybrid peptides (**P1**–**P3**) indicating the backbone expanded version of a 3$_{10}$-helix.[17b,21] In contrast to the average ϕ and ψ values of the 3$_{10}$-helix (−49°, −26°), L-Ala in the peptides **P2** and **P3** displayed the average ϕ and ψ values −68 ± 3° and −33.03 ± 3°, respectively. The torsional angles of all hybrid peptides are tabulated and given in the ESI.†. A plot of ϕ and ψ angles of all residues in peptides **P1**–**P3** is shown in Fig. 3a. Keeping θ_1 and θ_2 as constants, two distinct regions in the left quadrant of the Ramachandran map[18] can be recognised for γ- and α-residues.

In comparison between the α-residues in α/γ^4-hybrid peptides and 3$_{10}$-helix, a clear distinction can be observed particularly in the ϕ values. The L-Ala displayed an average of 10° higher value over the sterically constrained dialkyl amino acids in α/γ^4-hybrid peptides and an average of 19° over the α-residues in the 3$_{10}$-helix. The crystal structure results suggest that a stable 12-helix can be constructed using either the stereochemically constrained Aib or simple unconstrained α-residues in the combination with alternating γ^4-residues. Further, the top view of the 12-helices indicates the projections of the side chains at four corners of the helical cylinder (Fig. 2a, bottom plane). In comparison to the α-, β- and γ-peptides, the distinct orientation of the amino acid side-chains was observed in α/γ^4-hybrid 12-helices. Based on this information we predicted the helical wheel diagram for α/γ^4-hybrid peptide 12-helices (Fig. 3b). In hindsight, the analysis of the packing modes of all three peptide helices reveals the importance of proteinogenic amino acid side-chains. In contrast to **P1** and **P2**, **P3** with α-alanine residues showed the lateral interactions between the two anti-parallel helices. The packing of antiparallel helices is stabilized by the side-chain hydrophobic as well as CH···π interactions. The anti-parallel packing of **P3** is shown in Fig. 2b. These packing interactions may provide the guidance for structure based design from α/γ^4-hybrids to target protein structures. In addition two water molecules located at C- and

Table 1 Average helical parameters of backward 1←4 H-bonded helices

Peptide backbone	Res/ turn n	Rise/ turn p (Å)	Rise/ res d (Å)	Radius r (Å)
α/γ^4-Peptide (12-helix)	2.7	5.3	2.0	2.1
β-Peptide(*trans* ACPC)12-helix[a]	2.7	5.4	2.0	2.1
β-Peptide(*trans* ACBC)12-helix[b]	−2.7[d]	−5.4[d]	2.0	2.2
3_{10}-Helix[c]	3.2	5.8	1.8	2.0

[a] Ref. 8. [b] Ref. 7. [c] Ref. 21. [d] Negative sign indicates the left handed helical turn.

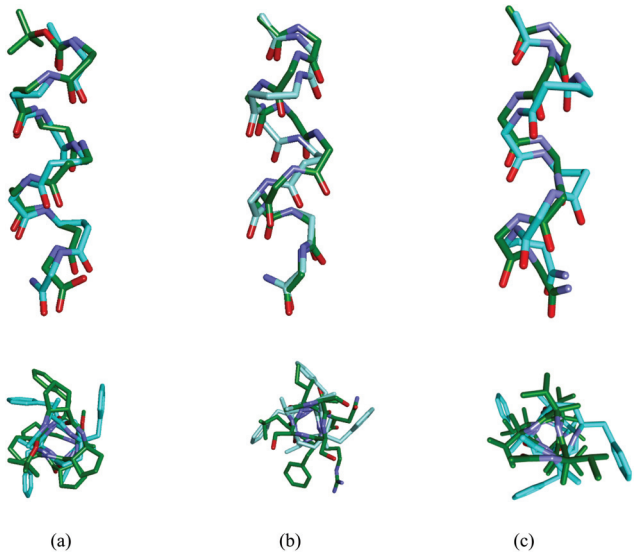

Fig. 4 Superposition of α/γ^4-hybrid peptide **P3** (light blue) on (a) β-peptide 12-helix, (b) α-helix and (c) 3_{10}-helix. The top view (lower plane) depicting the projection of amino acid side-chains.

N-terminals of the antiparallel helices play a crucial role in interconnecting the two helices.

Structural analogy with α-peptide helices, β-peptide 12-helices and helical parameter analysis

The intriguing results from the hybrid peptides **P1**, **P2** and **P3** encourage us to determine the helical parameters of α/γ^4-hybrid peptide 12-helices. The helical parameters were calculated from the set of four consecutive α-carbons using reported methods.[19] The analysis reveals all characteristic features such as residue-per-turn, rise-per-turn and the radius of α/γ^4-hybrid peptide 12-helix. The average helical parameters obtained from the three crystal structures are tabulated in Table 1. Recently, Gellman *et al.* reported the helical parameters for the β-peptide 12-helix[8] containing stereochemically constrained cyclic β-amino acids. Interestingly, the helical parameters calculated for the α/γ^4-hybrid peptides are in good agreement with the β-peptide12-helices [residue-per-turn (2.7), rise-per-turn (5.4 Å) and radius (2.1 Å)] generated from the cyclopentane backbone constraints. The overlay of the peptide **P3** on the β-peptide[8] 12-helix is shown in Fig. 4a. For comparison, the average structural parameters of β-peptide 12-helices and the 3_{10}-helix[21] are tabulated in Table 1. In addition, α/γ^4-hybrid peptide 12-helices displayed a very similar CD signature as that of β-peptide 12-helices with a CD maximum at 205 nm and a weak minimum at 218 nm (See ESI†).[20] The negative parameters of 12-helices generated from the cyclobutane ring constraints confirm the left-handed helical conformation of the β-peptide.[7] Further, we superimposed the α/γ^4-hybrid peptide **P3** over the α-helix and the 3_{10}-helix to understand the backbone correlation and the side-chain orientation as the H-bonding directionality of hybrid peptide 12-helices was very similar to that of α-peptide helices. The superposition of the backbone conformations of **P3** over the α-helix (from the protein Human DNA Polymerase Beta, PDB code – 1ZQA, sequence – 94–102)[22] and the 3_{10}-helix[23] is shown in Fig. 4b and 4c respectively. Similar to the α, γ^4-hybrid hexapeptide,[16b] the backbone conformation of the hybrid heptapeptide **P3** is well correlated with the nine residues of the α-helix. Instructively, a good backbone correlation of heptapeptide **P3** was observed with the heptapeptide 3_{10}-helix. The structures of the β-peptide 12-helix, α-helix and 3_{10}-helix were generated using the co-ordinates reported in the literature.[24] The top view of the superimposed **P3** with the α-helix and the 3_{10}-helix signifies the projection of the amino acid side-chains (Fig. 4, down plane). Similar results were also observed for the hybrid peptides **P1** and **P2** (data not shown). The backbone correlation and the side-chain projections of α/γ^4-hybrid peptide helices with respect to the α-helix suggest that these hybrid peptides can be exploited as mimics of α-peptide helices. Further, with the availability of broad side-chain diversity in both α- and γ^4-amino acids, these α/γ^4-hybrid peptides stand unique from the other α/γ-hybrid peptides. The structural analysis of α/γ-hybrid peptides containing backbone homologated γ^4-amino acids with proteinogenic side chains presented here may be useful for the design of functional foldamers similar to the β- and α/β-hybrid peptides.

Conclusion

In conclusion, we have presented the facile solid phase synthesis and single crystal conformations of α/γ^4-hybrid peptides. The stereochemical analysis suggests that all three α/γ^4-hybrid heptapeptides adopted 12-helical conformations in single crystals. Comparison between the **P1** and **P3** reveals that the 12-helical conformation can be induced in a hybrid peptide sequence solely through intramolecular H-bonding without using any stereochemical constraints. In addition, analogy with the β-peptide 12-helix suggests that α/γ^4-hybrid peptides can be used as surrogates of β-peptide 12-helices. Analysis of the helical parameters and the backbone correlation with the 3_{10}-helix suggests that the α/γ^4-hybrid peptide is comparable to an α-peptide helix except the projection of the amino acid side chains. The distinct location of the amino acid residues in the helical wheel diagram presented here may

be useful in the design of hybrid peptides with specific patterns. We believe that the facile protocol for the synthesis of γ^4-amino acids, crystal conformations of the hybrid peptides and their analogy with α- and β-peptide helices presented here may offer the guidelines to design α/γ^4-hybrid peptides with specific functions.

Experimental

Chemical synthesis of Fmoc-γ^4-Phe-OH

The suspension of activated Pd/C (20% by weight) and benzyl esters of N-Cbz-protected vinylogous phenylalanine (1.66 g, 4 mmol), which was synthesized using the reported method,[25] in 10% acetic acid in THF (20 mL) was stirred overnight at room temperature in the presence of hydrogen. After completion of the reaction, Pd/C was filtered through the bed of celite and the filtrate was evaporated to dryness under *vacuum* to get gummy free γ^4-phenylalanine (γ^4-Phe). The pure γ^4-Phe was isolated as a white powder after trituration with cold diethyl ether in excellent yield (0.687 g, 90%).

Further, to the solution of free γ^4-Phe (0.579 g, 3 mmol) in 20% Na_2CO_3 (15 mL) was added Fmoc-OSu (1.11 g, 3.3 mmol, dissolved in 10 mL of THF) and the reaction mixture was stirred overnight. After completion of the reaction, the reaction mixture was acidified with 10% HCl and the precipitated Fmoc protected γ^4-Phe was extracted with EtOAc (3 × 25 mL). The combined organic layer was washed with 10% HCl (3 × 15 mL), brine solution (2 × 10 mL), dried over Na_2SO_4 and concentrated under reduced pressure to give gummy Fmoc-γ^4-Phe. The gummy Fmoc-γ^4-Phe was precipitated using ethyl acetate/pet. ether (60–80 °C) to give 1.06 g (85%) as a white powder and used directly in the solid phase peptide synthesis.

Peptide synthesis

Peptides **P1**, **P2** and **P3** were synthesized by manual solid phase peptide synthesis on a Knorr Amide MBHA resin by Fmoc-chemistry (0.25 mmol scale). Coupling reactions were performed using the HBTU/HOBt/NMP activation protocol. Fmoc deprotections were facilitated by using 20% piperidine in DMF. N-terminal of peptides was capped with an acetyl group. Peptides were cleaved from the resin by using 95% trifluoroacetic acid, 2.5% water and 2.5% triisopropyl silane cleavage mixture. Reverse-phase-HPLC purification (detector: 254 nm and 220 nm) on a C_{18} column (70% methanol to 90% methanol in 40 min) at a flow rate of 1.5 mL min^{-1} was carried out to get pure peptides.

Crystal structure analysis

Crystal structure analysis of γ^4-Phe. Crystals of γ^4-Phe were grown by slow evaporation from a solution of aqueous methanol. A single crystal, rectangular in shape (0.50 × 0.40 × 0.20 mm^3) was mounted on a loop. The X-ray data were collected at 100(2) K temperature on a Bruker AXS SMART APEX CCD diffractometer using Mo-K_α radiation (λ = 0.71073 Å), ω-scans (2θ = 54.88°), for a total number of 8120 independent reflections. Space group *P*21; a = 7.757(5), b = 6.483(4), c = 9.907(7) Å; $\alpha = \gamma$ = 90.00°, β = 92.808(12) (3)°. V = 497.6(6) $Å^3$, monoclinic P; Z = 2 for chemical formula $C_{11}H_{15}N_1O_2$; ρ_{calcd} = 1.290 Mg m^{-3}; μ = 0.088 mm^{-1}; F (000) = 208. The structure was obtained by direct methods using SHELXS-97. All non-hydrogen atoms were refined anisotropically. The hydrogen atoms were fixed geometrically in the idealized position and refined in the final cycle of refinement as riding over the atoms to which they are bonded. The final R value was 0.0704 (wR_2 = 0.1626) for 2196 observed reflections ($F_0 \geq 4\sigma$ ($|F_0|$)) and 128 variables; S = 0.947. The largest difference peak and hole were 0.424 and −0.314 e $Å^{-3}$, respectively.

Crystal structure analysis of peptide P1. Crystals of α/γ^4-hybrid peptide **P1** were grown by slow evaporation from a solution of aqueous methanol–TFE. A single crystal, rectangular in shape (0.40 × 0.20 × 0.12 mm^3) was mounted on a loop. The X-ray data were collected at 100(2) K temperature on a Bruker AXS SMART APEX CCD diffractometer using Mo-K_α radiation (λ = 0.71073 Å), ω-scans (2θ = 56.50°), for a total number of 26 870 independent reflections. Space group *P*21; a = 12.866-(15), b = 17.403(19), c = 13.962(16) Å; $\alpha = \gamma$ = 90.00°, β = 107.22 (3)°. V = 2986(6) $Å^3$, monoclinic P; Z = 2 for chemical formula $C_{51}H_{72}N_8O_8$; ρ_{calcd} = 1.029 Mg m^{-3}; μ = 0.07 mm^{-1}; F (000) = 996. The structure was obtained by direct methods using SHELXS-97. All non-hydrogen atoms were refined anisotropically. The hydrogen atoms were fixed geometrically in the idealized position and refined in the final cycle of refinement as riding over the atoms to which they are bonded. The final R value was 0.0813 (wR_2 = 0.1855) for 13 302 observed reflections ($F_0 \geq 4\sigma$ ($|F_0|$)) and 596 variables; S = 0.733. The largest difference peak and hole were 0.213 and −0.239 e $Å^{-3}$, respectively.

Crystal structure analysis of peptide P2. Crystals of α/γ^4-hybrid peptide **P2** were grown by slow evaporation from a solution of aqueous methanol–TFE. A single crystal, rectangular in shape (0.40 × 0.30 × 0.20 mm^3), was mounted on a loop. The X-ray data were collected at 100(2) K temperature on a Bruker AXS SMART APEX CCD diffractometer using Mo-K_α radiation (λ = 0.71073 Å), ω-scans (2θ = 56.56°), for a total number of 24 197 independent reflections. Space group *P*1; a = 9.354(10), b = 12.179(13), c = 13.950(15) Å; α = 68.89 (3)°, β = 85.74 (3)°, γ = 71.36 (3)°, V = 1403(3) $Å^3$, triclinic P; Z = 1 for chemical formula $C_{48}H_{66}N_8O_8$, (O); ρ_{calcd} = 1.064 Mg m^{-3}; μ = 0.074 mm^{-1}; F (000) = 482. The structure was obtained by direct methods using SHELXS-97. All non-hydrogen atoms were refined anisotropically. The hydrogen atoms were fixed geometrically in the idealized position and refined in the final cycle of refinement as riding over the atoms to which they are bonded. The final R value was 0.0833 (wR_2 = 0.2342) for 10 395 observed reflections ($F_0 \geq 4\sigma$ ($|F_0|$)) and 569 variables; S = 0.771. The largest difference peak and hole were 0.056 and −0.257 e $Å^{-3}$, respectively.

Crystal structure analysis of peptide P3. Crystals of α/γ^4-hybrid peptide **P3** were grown by slow evaporation from a solution of aqueous methanol. A single crystal, rectangular in shape (0.40 × 0.29 × 0.16 mm^3), was mounted on a loop. The X-ray data were collected at 100(2) K temperature on a Bruker

AXS SMART APEX CCD diffractometer using Mo-K_α radiation (λ = 0.71073 Å), ω-scans (2θ = 56.56°), for a total number of 16 669 independent reflections. Space group *P*21; a = 11.218(17), b = 14.58(2), c = 15.75(2) Å; $\alpha = \gamma = 90°$, β = 100.06 (3)°, V = 2536(7) Å^3, monoclinic P; Z = 2 for chemical formula $C_{47}H_{64}N_8O_8$, 2(O); ρ_{calcd} = 1.140 Mg m^{-3}; μ = 0.079 mm^{-1}; F (000) = 924. The structure was obtained by direct methods using SHELXS-97. All non-hydrogen atoms were refined anisotropically. The hydrogen atoms were fixed geometrically in the idealized position and refined in the final cycle of refinement as riding over the atoms to which they are bonded. The final R value was 0.0824 (wR_2 = 0.1713) for 10 827 observed reflections ($F_0 \geq 4\sigma$ ($|F_0|$)) and 591 variables; S = 0.909. The largest difference peak and hole were 0.428 and −0.366 e Å^{-3}, respectively.

Acknowledgements

We thank the Department of Science and Technology, Government of India, for financial support. S.V.J. and A.B. are thankful to CSIR, India, for a Senior Research Fellowship.

References

1 (*a*) S. Jones and J. M. Thornton, *Proc. Natl. Acad. Sci. U. S. A.*, 1996, **93**, 13; (*b*) A. G. Cochran, *Curr. Opin. Chem. Biol.*, 2001, **5**, 654; (*c*) M. Guharoy and P. Chakrabarti, *Bioinformatics*, 2007, **23**, 1909; (*d*) D. P. Fairlie, M. W. West and A. K. Wong, *Curr. Med. Chem.*, 1998, **5**, 29; (*e*) R. Q. Lavery, *Rev. Biophys.*, 2005, **38**, 339; (*f*) D. E. Draper, *Annu. Rev. Biochem.*, 1995, **64**, 593.

2 (*a*) G. A. Woolley, *Acc. Chem. Res.*, 2005, **38**, 486; (*b*) K. Fujimoto, M. Kajino and M. Inouye, *Chem.–Eur. J.*, 2008, **14**, 857; (*c*) N. L. Mills, M. D. Daugherty, A. D. Frankel and R. K. Guy, *J. Am. Chem. Soc.*, 2006, **128**, 3496; (*d*) J. Garner and M. M. Harding, *Org. Biomol. Chem.*, 2007, **5**, 3577; (*e*) M. J. I. Andrews and A. B. Tabor, *Tetrahedron*, 1999, **55**, 11711.

3 A. Patgiri, A. L. Jochim and P. S. Arora, *Acc. Chem. Res.*, 2008, **41**, 1289.

4 C. G. Cummings and A. D. Hamilton, *Curr. Opin. Chem. Biol.*, 2010, **14**, 341.

5 (*a*) D. Seebach, A. K. Beck and D. J. Bierbaum, *Chem. Biodiv.*, 2004, **1**, 1111; (*b*) D. Seebach and J. Gardiner, *Acc. Chem. Res.*, 2008, **41**, 1366; (*c*) W. S. Horne and S. H. Gellmann, *Acc. Chem. Res.*, 2008, **41**, 1399; (*d*) P. G. Vasudev, S. Chatterjee, N. Shamala and P. Balaram, *Chem. Rev.*, 2011, **111**, 657; (*e*) L. K. A. Pilsl and O. Reiser, *Amino Acids*, 2011, **41**, 709; (*f*) S. Hanessian, X. Luo, R. Schaum and S. Michnick, *J. Am. Chem. Soc.*, 1998, **120**, 8569; (*g*) T. A. Martinek and F. Fulop, *Chem. Soc. Rev.*, 2012, **41**, 687; (*h*) E. J. Petersson and A. Schepartz, *J. Am. Chem. Soc.*, 2008, **130**, 821; (*i*) M. W. Giuliano, W. S. Horne and S. H. Gellman, *J. Am. Chem. Soc.*, 2009, **131**, 9860; (*j*) G. V. M. Sharma, V. B. Jadhav, K. V. S. Ramakrishna, P. Jayaprakash, K. Narsimulu, V. Subash and A. C. Kunwar, *J. Am. Chem. Soc.*, 2006, **128**, 14657; (*k*) J. L. Goodman, E. J. Petersson, D. S. Daniels, J. X. Qiu and A. Schepartz, *J. Am. Chem. Soc.*, 2007, **129**, 14746.

6 D. H. Appella, L. A. Christianson, I. L. Karle, D. R. Powell and S. H. Gellman, *J. Am. Chem. Soc.*, 1996, **118**, 13071.

7 C. Fernandes, S. Faure, E. Pereira, V. Thery, V. Declerck, R. Guillot and D. J. Aitken, *Org. Lett.*, 2010, **12**, 3606.

8 S. H. Choi, I. A. Guzei, L. C. Spencer and S. H. Gellman, *J. Am. Chem. Soc.*, 2010, **132**, 13879.

9 I. M. Mandity, L. Fulop, E. Vass, G. K. Toth, T. A. Martinek and F. Fulop, *Org. Lett.*, 2010, **12**, 5584.

10 (*a*) W. S. Horne, J. L. Price and S. H. Gellman, *Proc. Natl. Acad. Sci. U. S. A.*, 2008, **105**, 9151; (*b*) E. P. English, R. S. Chumanov, S. H. Gellman and T. Compton, *J. Biol. Chem.*, 2006, **281**, 2661.

11 Y. Imamura, N. Watanabe, N. Umezawa, T. Iwatsubo, N. Kato, T. Tomita and T. Higuchi, *J. Am. Chem. Soc.*, 2009, **131**, 7353.

12 S. Kwon, A. Jeon, S. H. Yoo, I. S. Chung and H.-S. Lee, *Angew. Chem., Int. Ed.*, 2010, **49**, 8232.

13 C. Baldauf, R. Gunther and H.-J. Hofmann, *J. Org. Chem.*, 2006, **71**, 1200.

14 (*a*) S. Chatterjee, P. G. Vasudev, S. Raghothama, C. Ramakrishnan, N. Shamala and P. Balaram, *J. Am. Chem. Soc.*, 2009, **131**, 5956; (*b*) K. Basuroy, B. Dinesh, N. Shamala and P. Balaram, *Angew. Chem., Int. Ed.*, 2012, **51**, 8736.

15 (*a*) L. Guo, W. Zhang, I. A. Guzei, L. C. Spencer and S. H. Gellman, *Org. Lett.*, 2012, **14**, 2582; (*b*) L. Guo, Y. Chi, A. M. Almeida, I. A. Guzei, B. K. Parker and S. H. Gellman, *J. Am. Chem. Soc.*, 2009, **131**, 16018.

16 (*a*) A. Bandyopadhyay and H. N. Gopi, *Org. Lett.*, 2012, **14**, 2770; (*b*) A. Bandyopadhyay, S. V. Jadhav and H. N. Gopi, *Chem. Commun.*, 2012, **48**, 7170.

17 (*a*) C. Toniolo and E. Benedetti, *Trends Biochem. Sci.*, 1991, **16**, 350; (*b*) I. L. Karle and P. Balaram, *Biochemistry*, 1990, **29**, 6747.

18 G. N. Ramachandran and V. Sasisekharan, *Adv. Protein Chem.*, 1968, **23**, 283.

19 (*a*) H. Sugeta and T. Miyazawa, *Biopolymers*, 1967, **5**, 673; (*b*) M. Bansal, S. Kumar and R. Velavan, *J. Biomol. Struct. Dyn.*, 2000, **17**, 811.

20 J. S. Park, H. S. Lee, J. R. Lai, B. M. Kim and S. H. Gellman, *J. Am. Chem. Soc.*, 2003, **125**, 8539.

21 D. J. Barlow and J. M. Thornton, *J. Mol. Biol.*, 1988, **201**, 601.

22 H. Pelletier and M. R. Sawaya, *Biochemistry*, 1996, **35**, 12778.

23 C. Crisma, M. Saviano, A. Moretto, Q. B. Broxterman, B. Kaptein and C. Toniolo, *J. Am. Chem. Soc.*, 2007, **129**, 15471.

24 The overlayed structures of β-peptide 12-helix, α-helix and 3_{10}-helix were generated from crystal co-ordinates reported in ref. 8, 22 and 23 respectively.

25 S. M. Mali, A. Bandyopadhyay, S. V. Jadhav, M. G. Kumar and H. N. Gopi, *Org. Biomol. Chem.*, 2011, **9**, 6566.

